Chemical functionalization of carbon nanotubes through energetic radical collisions

Boris Ni and Susan B. Sinnott*

The University of Kentucky, Department of Chemical and Materials Engineering, Lexington, Kentucky 40506

(Received 1 February 2000)

Classical molecular dynamics simulations are used to model the bombardment of a bundle of single walled carbon nanotubes by CH_3 radicals impacting with incident energies of 10, 45, and 80 eV. The simulations show that there is a high probability of adhesion of either the radicals or their fragments to the nanotube walls at all the incident energies considered. They therefore predict a pathway to the chemical functionalization of the walls of carbon nanotubes. The simulations also show how at 80 eV the incident radicals can induce cross-linking between the nanotubes.

Carbon nanotubes are being considered for use as fibers in the next generation of composite materials. Sometimes fibers are chemically functionalized with polymer chains to increase their adhesion to the polymer matrix in a composite.[1] Creation of covalent, nonplanar C-C bonds to the walls of carbon nanotubes results in the breaking of the local sp^2 hybridization and the formation of π-π conjugated bonds at the surface of the nanotube. Calculations of the chemical functionalization of single-walled nanotubes (SWNT's) predict that functionalization decreases the Young's modulus of the nanotubes by about 15%,[2] and can alter their electronic structure.[3] Recent experiments have succeeded in functionalizing SWNT's at their open ends[4,5] and at the walls[5,6] by using carbodiimide chemistry[4] or mixing the nanotubes with an electrophilic reagent that adds to deactivated double bonds.[5,6]

The objective of this work is to investigate a different route for chemical functionalization of SWNT walls by radical bombardment. Simulations to study the creation of ''nanogears'' through the collision of benzene radicals with a SWNT have been considered previously,[7] but only under idealized conditions to show that it was possible to attach a benzyl radical to a nanotube wall. No extensive studies over a range of incident energies on more than one SWNT have yet been undertaken. It is to be expected that radical collisions at hyperthermal energies could also create defects in the walls of the SWNT's similar to those observed during electron irradiation of nanotubes.[8] Therefore, the second goal of this work is to study the creation or removal of defects through radical collisions and determine their dependence on the radicals' incident energy. The impacts of energetic radicals with the capped ends of the nanotubes are also considered to compare the reactions at the caps to those that occur at the walls. Finally, the effects of 5/7 defects already present within the nanotube walls on the results of the collisions are examined. The approach in this study is classical molecular dynamics simulations.

The simulations use a third-order Nordsieck predictor corrector routine[9] to integrate Newton's equation of motion with a time step of 0.20 femtoseconds (fs). The forces on all the atoms are calculated using an analytic reactive empirical bond-order potential (REBO) developed by Brenner[10,11] coupled to a long-range Lennard-Jones potential as described in detail elsewhere.[12] This many-body potential has been successfully applied to model the related processes of ion bombardment of polymer surfaces[13] and thin-film growth through molecular and cluster beam deposition.[11] It has also been used extensively to study the mechanical properties of carbon nanotubes.[14–16] In most cases, this potential has been shown to provide reasonable predictions.[12] However, as is the case for all empirical potentials, there are cases where the quantitative accuracy is lacking even while the qualitative trends are correct. For example, Hase and co-workers[17] have shown that the REBO potential predicts association potentials for $H+CH_3$ and H+diamond (111) that are significantly smaller than *ab initio* values because of the potential's shorter range. Within the REBO potential cutoff, the predicted association potentials are similar to the *ab initio* values.[17] Therefore, this effect is not of significant concern in the present study because of the relatively high incident energies used that bring the radicals into close contact with the nanotube walls (well within the potential cutoff) prior to any reaction.

The system used in the simulations consists of a bundle of six (10,10) SWNT's arranged in two layers as shown in Fig. 1. Each SWNT is 50 Å long and consists of 800 atoms. Periodic boundary conditions[9] are applied within the plane of the nanotubes, perpendicular to the direction of collision onto the nanotube walls. At the nanotube edges, 20 atoms are held rigid (not allowed to evolve in time) throughout the

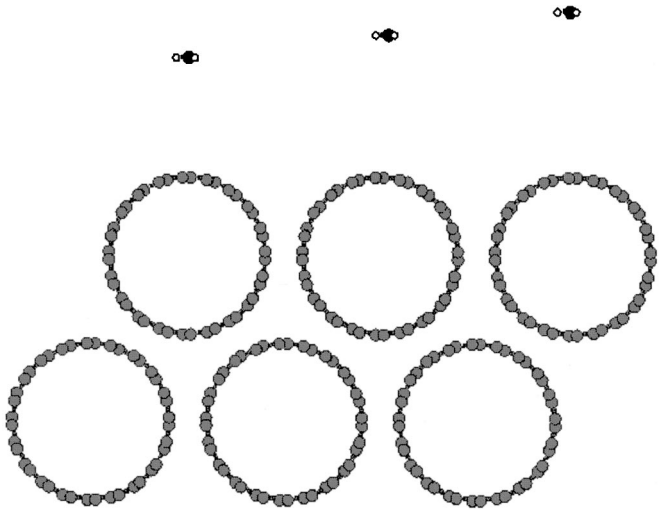

FIG. 1. Snapshot of the initial conditions of the impact simulations. The gray spheres represent nanotube carbon atoms, black spheres represent carbon in the incident CH_3 radicals, and white spheres represent hydrogen in the CH_3 radicals.

TABLE I. Percentage of events taking place in collisions of CH_3 with a bundle of (10,10) single-walled carbon nanotubes. The data are the averages of the outcomes of 35 trajectories (105 collisions) performed for each incident energy.

	10 eV	45 eV	80 eV
Scattering of CH from nanotubes		6.7	1.3
Scattering of CH_2 from nanotubes		9.3	2.7
Scattering H from nanotubes		53.6	66.3
Scattering of CH_3 from nanotubes	24.0	8.0	4.0
Adsorption of C, outside wall			26.7
Adsorption of C, in inside wall			26.7
Adsorption of CH, outside wall		28.0	10.7
Adsorption of CH_2, outside wall		24.0	4.0
Adsorption of CH_3, outside wall	76.0	5.3	
Defects structures form		18.7	24.0
Adsorption of H, outside wall		14.2	23.2
Adsorption of H, inside wall			3.2

simulations. Moving towards the center of the nanotubes, 40 atoms have Langevin frictional forces[9] applied to them to maintain the temperature at 300 K. The other atoms in the system are allowed to evolve in time with no constraints. Another configuration was also considered where none of the atoms are held rigid and 140 atoms at the nanotube ends have Langevin frictional forces applied to them. The results from the two configurations showed negligible differences.

Every trajectory involved the bombardment of three CH_3 radicals initially positioned 10, 12, and 14 Å above the top three SWNT's as shown in Fig. 1. The radicals were then given incident energies towards the nanotubes. The trajectories ran until it was clear the results were not going to change, with most lasting about 800 fs. Three incident energies of 10, 45, and 80 eV were considered and 35 trajectories (105 impacts) were performed for each incident energy from slightly different starting conditions obtained by varying the positions of the incident CH_3 radicals relative to the nanotubes. Some of the starting conditions place the radicals directly above the center of the nanotubes (as shown in Fig. 1) while some position the radicals to impact the nanotubes along their sides.

The simulation results are presented in Table I. At incident energies of 10 eV only two kinds of phenomena are predicted to occur. The first is the scattering of CH_3 radicals from the nanotube bundle while the second is the adsorption of the fragments on the outer walls of the carbon nanotubes at the first site they hit, as shown in Fig. 2(a). Adhesion is predicted to occur more often as most of the time the impacting radicals impact onto or very near a C atom on the nanotube wall. The final length of the C-C bond formed between the nanotube wall and the CH_3 is about 1.55 Å, a value that is quite close to normal C-C bond lengths in alkanes. Before the collision the C-C bond lengths in the nanotube wall are around 1.42 Å while after adsorption the C-C bond lengths in the nanotube wall around the adsorption site are about 1.55 Å.

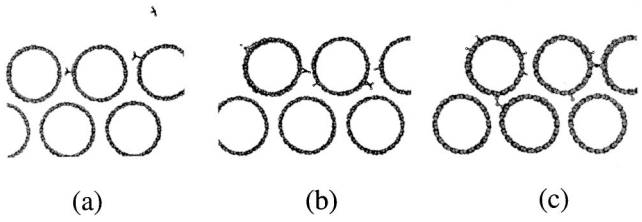

FIG. 2. Representative snapshots of collision outcomes for CH_3 impacting at (a) 10 eV, (b) 45 eV, (c) 80 eV. The color scheme is the same as in Fig. 1.

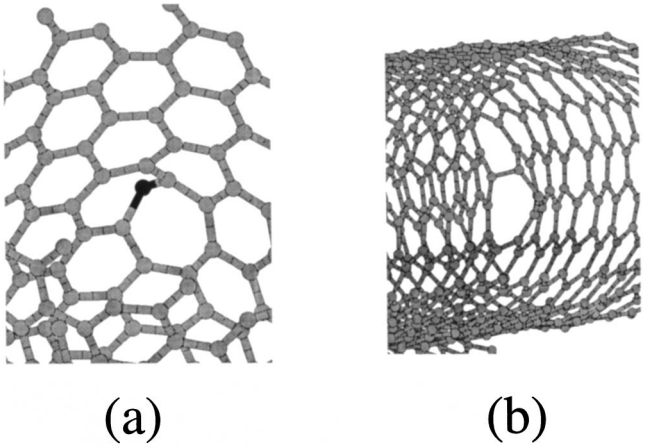

FIG. 3. Examples of defects formed from CH_3 impacting at (a) 45 eV and (b) 80 eV. The color scheme is the same as in Fig. 1.

At incident energies of 45 eV only about 13% of the CH_3 radicals remain intact after the collisions and only 8% scatter away intact. Most of the radicals break apart on impact and the larger fragments, such as CH and CH_2, adsorb on the outer surface of the nanotubes in about 52% of the collisions. In some cases, fragments such as CH_2 and CH create two or, more rarely, three covalent bonds with surface atoms, as shown in Fig. 2(b). Generally these fragments do not bond to the first carbon atom they hit, but rather move along the nanotube making contact with 2–3 carbon atoms before finally bonding to the nanotube wall. Most of the H atoms knocked loose on impact scatter away from the nanotubes although some adsorb to the outer wall.

The collisions at 45 eV also cause defects to form in the nanotube walls. However, the nanotube atoms usually reform their original bonding configuration in the course of the simulation. In about 2% of the collisions, carbon atoms were knocked out of the nanotube walls by the CH_3 creating permanent vacancies in the nanotubes. It should be emphasized that each nanotube is only struck by one radical per trajectory in the simulations, and therefore the same ability to reconstruct might not occur during bombardment if the time between subsequent hits is less then the time of recreation. Another defect observed in about 19% of collisions is the insertion of the carbon atom from the CH_3 into the nanotube structure. In these cases the defect takes the form of two conjugated heptagons that slightly deform the outer surface of the affected SWNT as shown in Fig. 3(a). It has been recently shown that bent nanotubes have enhanced reactivity.[18] Therefore these defect centers could, in their turn, serve as centers of enhanced reactivity and functionalization for future impacts.

At 80 eV, most CH_3 radicals are completely broken apart and only 4% of them scatter away intact. Furthermore, the impacts at these energies are so severe that the amplitude of

local deformation within the nanotubes can reach $\frac{1}{3}$ of the nanotube's diameter. The largest fragments from the CH_3 radicals adsorb on the nanotube walls and most of the hydrogen atoms scatter away from the nanotubes. However, in contrast to what was seen previously at 45 eV, the fragments are mostly lone atoms [see Fig. 2(c)]. Again, the fragments make contact with 2–3 carbon atoms in the nanotube wall before adhering to one of them. About 15% of the time the incident CH_3 radicals knock out one or more carbon atoms from the walls creating large holes that do not heal on the time scales on these simulations, as shown in Fig. 3(b). Incident C atoms can also insert into the nanotube structure creating various complexes of pentagons, heptagons, and octagons.

In contrast to what was seen at the lower incident energies, about 27% of the carbon atoms from the CH_3 radicals knock out other C atoms from the nanotube walls. This usually happens when the impacting radical hits directly on or very close to an individual carbon atom on the wall. In some cases, the C from the CH_3 substitutes for the knocked out atom. In addition, the knocked-out atom sometimes reacts with the atoms on the interior far wall. The knocked-out atom can also knock out another atom on the far wall which then goes on to adhere to a nanotube in the second layer of the bundle. None of the simulations predict that a C atom from an incident CH_3 penetrates directly through the nanotube wall.

The interior bonding sites were predicted to be potential energy minima in Ref. 19. The REBO potential predicts that adhesion of single C atoms to the exterior of a (10,10) nanotube is more stable than adhesion to the interior by 0.027 eV/atom. The simulations also predict cross-linking between the SWNT's in the bundle through bombardment at 80 eV, as illustrated in Fig. 2(c). This could toughen the nanotube bundle structure and stabilize it to shear in a manner that is analogous to the toughening of polymers by cross-linking the first few layers through ion bombardment.[20] The C-C bond lengths of the interconnecting segments vary from 1.55 to 1.72 Å.

To determine the effect of 5/7 defects on the results we considered the impact of CH_3 radicals on nanotubes that already had 5/7 defects present in the walls. Ten trajectories (30 impacts) on or around the 5/7 defects on the nanotubes in the bundle were performed. The most interesting effect predicted was the healing of the 5/7 defect when the CH_3 radical impacted at incident energies of 45 eV (in about 7% of the collisions) and 80 eV (in 10% of the collisions). This defect healing is shown in Fig. 4 for a collision at 45 eV and only happened for impacts that occurred directly on the defect. Otherwise, the outcomes of the collisions were very similar to those predicted for regular nanotubes.

Since experimental samples may not be perfectly aligned during bombardment, we also studied the impact of CH_3 radicals on the capped portions of capped (10, 10) SWNT's. Three trajectories were performed at every energy and each trajectory involved six CH_3 radicals impacting six capped nanotubes from slightly different initial positions (for a total of 18 collisions per incident energy). The simulations predict that the cap ends are even more flexible than the SWNT walls, a result that is compatible with the results of previous simulations on nanotube indentation.[14] At incident energies

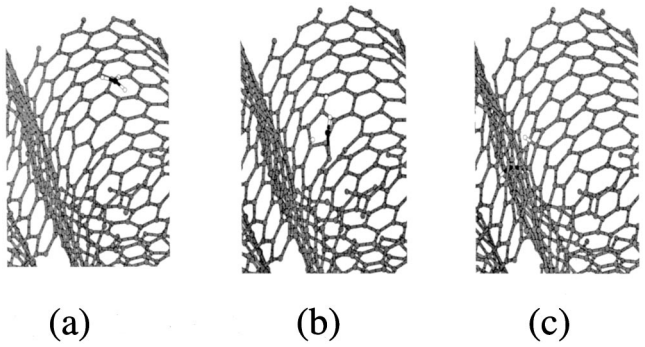

FIG. 4. Sequence showing an incident CH_3 impacting a nanotube with a 5/7 defect: (a) initial collision of the radical with the nanotube wall, (b) temporary bonding of the C from the radical to atoms in the 5/7 defect, (c) final structure—the 5/7 defect has been removed and the incident C atom is bonded to the side of where the defect used to be. The color scheme is the same as in Fig. 1.

of 10, 45, and 80 eV, 50%, 67%, and 33% of impacting CH_3 fragments, respectively, scatter away intact without affecting the bonding in the cap. Several vacancies and defect structures are formed within the cap at impacts of 45 eV (in about 17% of the collisions) and 80 eV (in about 83% of the collisions) because of the energy transferred to the impact site. At 10 eV, 50% of the collisions result in CH_3 bonding to the outside of the cap, which is in contrast to the much higher value of 76% for the nanotube wall. At 45 eV, 33% of the collisions result in CH fragments bonding to the outside of the cap, which is close to the 28% that adhere to the nanotube wall. However, no CH_2 or CH_3 fragments bond to the cap, in contrast to what occurs on nanotube walls. At 80 eV, C, CH, and CH_2 bond to the outside of the nanotube caps in 17%, 17%, and 33% of the collisions, respectively. In contrast, these species adhere to the outside walls in about 27%, 11%, and 4% of the collisions, respectively. In addition, about 27% of the fragments adhere to the inside walls at incident energies of 80 eV. Thus, there are differences in reactivity at the cap and the wall. These simulations predict that chemical functionalization of nanotube cap ends by energetic radical bombardment is less effective than chemically functionalizing the nanotube walls at the two lower incident energies.

To summarize, atomistic simulations have been performed to model the bombardment of a nanotube bundle with CH_3 radicals at incident energies of 10, 45, and 80 eV. They show the chemical adhesion of radicals or heavy fragments from the radicals, such as CH_2, CH, or C, to the SWNT's can occur at all the incident energies considered. The results also predict that this method of functionalization is more effective on the nanotube walls than on the caps at incident energies of 10 and 45 eV. Most of the hydrogen atoms that are knocked loose from the radicals on impact simply scatter away, although some adhere to the nanotubes. At incident energies of 45 and 80 eV, the impacts can also create defects and vacancies within the nanotube walls. When 5/7 defects are already present in the nanotube walls, the impact of the incident radicals can remove the defects. At 80 eV, the simulations also predict that the nanotube bundle can be cross-linked in a manner similar to that seen in polymers following ion bombardment.

This work was supported by the NSF (CHE-9708049) and (MRSEC-DMR-9809686) and by the NASA Ames Research Center (NAG 2-1121).

*Corresponding author.

[1] See, for example, R. Lin, R. P. Quirk, J. Kuang, and L. S. Penn, J. Adhes. Sci. Technol. **10**, 241 (1996).
[2] A. Garg and S. B. Sinnott, Chem. Phys. Lett. **295**, 273 (1998).
[3] D. W. Brenner *et al.*, J. Br. Interplanet. Soc. **51**, 137 (1998).
[4] J. Liu *et al.*, Science **280**, 1253 (1998).
[5] J. Chen *et al.*, Science **282**, 95 (1998).
[6] S. S. Wong *et al.*, Nature (London) **394**, 52 (1998).
[7] J. Han, A. Globus, R. Jaffe, and G. Deardorff, Nanotechnology **8**, 95 (1997).
[8] P. M. Ajayan, V. Ravikumar, and J.-C. Charlier, Phys. Rev. Lett. **81**, 1437 (1998).
[9] M. P. Allen and D. J. Tildesley, *Computer Simulation of Liquids* (Oxford University Press, New York, 1987).
[10] D. W. Brenner, Phys. Rev. B **42**, 9458 (1990).
[11] S. B. Sinnott, L. Qi, O. A. Shenderova, and D. W. Brenner, in *Molecular Dynamics of Clusters, Surfaces, Liquids, and Interfaces*, edited by W. Hase (JAI Press, Inc., Stamford, CT, 1999), pp. 1–26.
[12] Z. Mao, A. Garg, and S. B. Sinnott, Nanotechnology **10**, 273 (1999).
[13] D. W. Brenner, O. A. Shenderova, and C. B. Parker, Mater. Res. Soc. Symp. Proc. **438**, 491 (1997).
[14] A. Garg, J. Han, and S. B. Sinnott, Phys. Rev. Lett. **81**, 2260 (1998).
[15] B. I. Yakobson, C. J. Brabec, and J. Bernholc, Phys. Rev. Lett. **76**, 2511 (1996).
[16] C. F. Cornwell and L. T. Wille, Solid State Commun. **101**, 555 (1997).
[17] P. De Sainte Claire, K. Son, W. L. Hase, and D. W. Brenner, J. Am. Chem. Soc. **100**, 1761 (1996).
[18] D. Srivastava *et al.*, J. Phys. Chem. B **103**, 4330 (1999).
[19] A. A. Farajian *et al.*, J. Chem. Phys. **111**, 2164 (1999).
[20] E. H. Lee, G. R. Rao, M. B. Lewis, and L. K. Mansur, Nucl. Instrum. Methods Phys. Res. B **74**, 326 (1993).